Evidence for temperature-mediated regional increases in cerebral blood flow during exercise

Caldwell, Hannah; Coombs, Geoff; Howe, Connor; Hoiland, Ryan L; Patrician, Alexander; Lucas, Sam; Ainslie, Philip N

DOI:
10.1113/JP278827

Evidence for Temperature-Mediated Regional Increases in Cerebral Blood Flow during Exercise

Hannah G. Caldwell[1*], Geoff B. Coombs[1], Connor A. Howe[1], Ryan L. Hoiland[1], Alexander Patrician[1], Samuel J.E. Lucas[2], Philip N. Ainslie[1]

[1]*Centre for Heart, Lung and Vascular Health, School of Health and Exercise Sciences, University of British Columbia Okanagan, Kelowna, BC, Canada*

[2]*School of Sport, Exercise and Rehabilitation Sciences & Centre for Human Brain Health, University of Birmingham, Birmingham, United Kingdom*

Corresponding author: Hannah G. Caldwell, Centre for Heart, Lung and Vascular Health, School of Health and Exercise Sciences, University of British Columbia – Okanagan, 3333 University Way, Kelowna, British Columbia, Canada, V1V 1V7

Email address: hannahcaldwell@alumni.ubc.ca

Key Points:

- Aerobic exercise elicits increases in cerebral blood flow (CBF) as well as core body temperature; however, the isolated influence of temperature on CBF regulation during exercise has not been investigated
- This study assessed CBF regulation and neurovascular coupling during submaximal cycling exercise and temperature-matched passive heat stress during isocapnia (i.e., end-tidal PCO_2 was held constant)
- Submaximal cycling exercise and temperature-matched passive heat stress provoked approximately 16% increases in vertebral artery blood flow, independent of changes in end-tidal PCO_2 and blood pressure
- External carotid artery blood flow increased by approximately 43% during both exercise and passive heat stress with no change in internal carotid artery blood flow
- Neurovascular coupling (i.e., the relationship between local increases in cerebral metabolism and appropriately matched increases in regional cerebral blood flow) is preserved during both exercise and temperature-matched passive heat stress

ABSTRACT

Acute moderate-intensity exercise increases core temperature (Tc; +0.7-0.8°C); however, such exercise increases cerebral blood flow (CBF; +10-20%) mediated via small elevations in arterial PCO_2 and metabolism. This study aimed to isolate the role of Tc from PCO_2 on CBF regulation during submaximal exercise. Healthy adults (n=11; 10M/1F; 26±4 years) participated in two interventions each separated by ≥48 hours: 1) 60 mins semi-recumbent cycling (EX; 50% workload max); and 2) 75 mins passive heat stress (HS; 49°C water-perfused suit) to match the exercise-induced increases in Tc (EX: Δ0.75±0.33°C vs. HS: Δ0.77±0.33°C, P=0.855). Blood flow (Q) in the internal and external carotid (ICA and ECA, respectively) and vertebral (VA) arteries (Duplex ultrasound) was measured. End-tidal PCO_2 and PO_2 were effectively clamped to resting values within each condition. The Q_{ICA} was unchanged with EX and HS interventions (P=0.665), consistent with the unchanged end-tidal PCO_2 (P=0.327); whereas, Q_{VA} was higher throughout both EX and HS (EX: Δ16±21% vs. HS: Δ16±23%, time effect: P=0.006) with no between condition differences (P=0.785). These increases in Q_{VA} contributed to higher global CBF throughout both EX and HS (EX: Δ12±20% vs. HS: Δ14±14%, time effect: P=0.029; condition effect: P=0.869). The Q_{ECA} increased throughout both EX and HS (EX: Δ42±58% vs. HS: Δ53±28%, time effect: P<0.001; condition effect: P=0.628). Including blood pressure as a covariate did not alter these CBF findings (all P>0.05). Overall, these data provide new evidence for temperature-mediated elevations in posterior CBF during exercise that are independent of changes in PCO_2 and blood pressure.

INTRODUCTION

With relative increases in exercise intensity up to approximately 60-70% maximal oxygen uptake ($\dot{V}O_{2max}$), cerebral blood flow (CBF) increases progressively (+10-20%) (Ogoh & Ainslie 2009a; Sato & Sadamoto 2010) to regulate cerebral substrate delivery (Ide & Secher 2000; Fisher et al. 2013), and is mediated via relative alveolar hypoventilation (i.e., small elevations in arterial PCO_2; $PaCO_2$) and increases in cerebral oxidative metabolism ($CMRO_2$) (Nybo *et al.*, 2002; Smith *et al.*, 2014). Global CBF (*g*CBF) regulation during exercise and passive heat stress are both severity-dependent such that high-intensity exercise (e.g., >70% VO_{2max}) (Larsen *et al.*, 2008; Smith *et al.*, 2014) and severe passive heat stress (e.g., >1°C core temperature; Tc) both attenuate the elevated CBF via hyperventilatory-induced reductions in $PaCO_2$ (i.e., hypocapnia) to provoke cerebral vasoconstriction. Further, hypocapnic cerebral vasoconstriction uncouples appropriate changes in CBF to support local cerebral metabolism (i.e., neurovascular coupling; NVC) (Szabo *et al.*, 2011), and may explain previously observed regional differences in CBF with both exercise and passive heat stress (Sato *et al.*, 2011; Qian *et al.*, 2014; Smith *et al.*, 2016). With heavy aerobic exercise (i.e., 80% VO_{2peak}) (Sato *et al.*, 2011) – and related increases in Tc – and during passive heat stress (i.e., +1.5°C) (Ogoh *et al.*, 2014), internal carotid artery blood flow (Q_{ICA}) is reportedly compromised while blood supply to the face and neck is increased (e.g., *exercise:* +100% and *heat stress:* +130%, respectively) via redistribution of flow to the external carotid artery (Q_{ECA}) to aid thermoregulatory heat dissipation (Ogoh *et al.*, 2013; Sato *et al.*, 2016). These reductions in Q_{ICA} are likely explained by hypocapnia-mediated differences in vascular resistance of the ICA and ECA to regulate CBF (Sato *et al.*, 2011; Willie & Ainslie, 2011) as explained by a partial (Brothers *et al.*, 2009) or full restoration of Q_{ICA} (Nelson *et al.*, 2011; Bain *et al.*, 2013) when hypocapnia is acutely restored or when hyperventilation is voluntarily suppressed (Fujii *et al.*, 2015; Tsuji *et al.*, 2019).

The coupling between regional CBF and metabolism (i.e., NVC) allows for regulation of cerebral perfusion and temperature (Yablonskiy *et al.*, 2000). During exercise, *g*CBF is affected by the balance between contributions of cerebrovascular tone and perfusion pressure and is regulated via changes in $PaCO_2$, cerebral neural activity, and metabolism (i.e., $CMRO_2$) (Ogoh & Ainslie, 2009). Acute moderate-intensity exercise (e.g., 30-45 mins at 50-60% workload max) also increases Tc (e.g., *active* heat stress; +0.7-0.8°C) (Nybo *et al.*, 2002; Sato *et al.*, 2016), and

this elevation in Tc influences key CBF regulatory pathways (e.g., vascular tone, ventilatory control, and MAP). For example, *g*CBF *decreases* by 10-15% for every 1°C rise in Tc during *passive* heat stress, mediated via hyperventilatory-evoked reductions in $PaCO_2$ (Fan *et al.*, 2008; Bain *et al.*, 2013; Ogoh *et al.*, 2013; 2014; Bain *et al.*, 2015). Importantly, +2°C increase in Tc with passive heat stress provokes a 20% increase in $CMRO_2$ in humans, irrespective of the hyperthermic ventilatory response and resultant respiratory alkalosis (Bain et *al.*, 2019; in review). Further, when $PaCO_2$ was restored at +2°C Tc, $CMRO_2$ remained elevated with a respective *increase* in global CBF from normothermic values (Bain *et al.*, 2019; in review). As such, conceivable temperature-mediated increases in $CMRO_2$ – evoked via exercise or passive heat stress – may elicit related increases in CBF via the thermodynamic Q_{10} effect, independent of $PaCO_2$. Whether temperature *per se* influences CBF during exercise has not been investigated; therefore, we aimed to address this by using a temperature-matched passive heat stress protocol.

The purpose of this study was to investigate the influence of core temperature on cerebrovascular blood flow regulation in the ICA, ECA, and vertebral artery (VA), as well as NVC in the middle and posterior cerebral artery (MCA & PCA, respectively) during acute submaximal exercise, independent of changes in end-tidal PCO_2 ($P_{ET}CO_2$). We hypothesized that: 1) Blood flow in the ICA would be *maintained* during both exercise and passive heat stress with isocapnia, irrespective of competing increases in Q_{ECA}; 2) Blood flow in the ECA would be *increased* to the same extent with both temperature-matched exercise and passive heat stress for thermoregulatory heat dissipation; 3) Blood flow in the VA would be *increased* during both exercise and passive heat stress; 4) The NVC response would not be different between exercise and passive heat stress at matched temperature and $P_{ET}CO_2$.

METHODS

Eleven healthy young volunteers (n = 10 males/1 female; 26±4 years, 181±5 cm, 75±10 kg, 23±3 kg/m^2) were recruited to participate in this study. The female participant was taking an oral contraceptive and was tested within the early follicular phase (e.g., days 1 & 3). Participants had no history of cerebrovascular, cardiovascular, or respiratory disease and were not taking any prescription medication at their time of participation, as determined by a pre-screening questionnaire. Following verbal and written explanation of the study, written informed consent

was provided by all participants. This study was approved by the University of British Columbia Clinical Research Ethics Board (H17-02594) and all procedures were conducted in accordance with the Declaration of Helsinki, except registration in a database.

Experimental Protocol

Each experimental session was separated by at least 48 hours and was conducted at the same time of day. Participants refrained from alcohol and caffeine consumption as well as vigorous exercise or activity for at least 12 hours prior to experimental testing. Upon arrival to the laboratory, urine specific gravity (model TS 400, Reichert Analytical Instruments, Depew, NY, USA) was assessed to confirm adequate (≤1.020) hydration.

First, participants completed a peak oxygen consumption ($\dot{V}O_{2peak}$) exercise test on a semi-recumbent cycle ergometer (Angio 917900, Lode, Netherlands) to determine peak power output. Following 2.5 mins warm-up at 100 W, a ramp protocol was performed whereby cycling resistance was progressively increased by 1 W/ 3 sec (20 W/min) while participants maintained a self-selected cadence (70-80 rpm) until 1 of 2 criteria was met: 1) The participant no longer wished to continue (volitional exhaustion); 2) The participant was no longer capable of maintaining the required pedalling frequency (physical exhaustion).

Participants completed two experimental interventions, each separated by ≥48 hours: 1) 60 mins semi-recumbent cycling (EX; 50% workload max); and 2) 75 mins semi-recumbent passive heat stress (HS; 49°C water-perfused suit) to target the matched increases in Tc experienced during exercise. Cardiorespiratory, cerebrovascular, and thermometry variables were assessed before EX and HS bouts during thermoneutral rest (PRE). These variables were then assessed following approximately 45-60 mins of these conditions *during* EX and HS once Tc increases were matched and $P_{ET}CO_2$ had been effectively clamped to resting poikilocapnic levels for ≥5 mins. This steady-state restoration of $P_{ET}CO_2$ was maintained throughout the cerebrovascular assessment and has previously been shown to elicit an end-tidal to arterial PCO_2 gradient of approximately <1 mmHg (Tymko *et al.*, 2016). The order of acquisition of the extracranial arteries (e.g., common carotid artery, CCA; ICA; ECA; and VA) was randomized between participants and the order of CBF versus NVC assessment was counter-balanced between participants.

Cardiorespiratory Measures

Beat-by-beat blood pressure was acquired using non-invasive finger photoplethysmography (Finometer PRO, Finapres Medical Systems, Amsterdam, Netherlands) and was calibrated prior to data collection using the return-to-flow function. The Finometer blood pressure waveform was averaged to calculate MAP after calibrating values to the average of at least two automated brachial blood pressure measurements (Omron Healthcare, model: BP769CAN). Stroke volume (SV) was estimated from the blood pressure waveform (Beat Scope, Finapres Medical Systems, Amsterdam, Netherlands). Heart rate (HR) was continuously measured using a lead-II electrocardiogram (ECG; ADI BioAmp ML132).

Breath-by-breath CO_2 and O_2 were sampled at the mouth and recorded using a calibrated gas analyzer (model ML206, ADInstruments). The partial pressures of end-tidal CO_2 and O_2 (i.e., $P_{ET}CO_2$ and $P_{ET}O_2$, respectively) were calculated in LabChart using peak detection analysis with correction for daily barometric pressure. Both $P_{ET}CO_2$ and $P_{ET}O_2$ were controlled using a custom-designed dynamic end-tidal forcing system to effectively regulate end-tidal gases across wide ranges of $P_{ET}CO_2$ and $P_{ET}O_2$ independent of ventilation ($\dot{V}_E$); this device has previously been described in detail elsewhere (Tymko *et al.*, 2015; 2016). This was used to "clamp" $P_{ET}CO_2$ to poikilocapnic resting levels during EX and HS measures (i.e., conditions were isocapnic). Lastly, respiratory flow was measured by a pneumotachograph (model HR 800L, HansRudolph, Shawnee, KS, USA).

Cerebrovascular Measures

Transcranial Doppler (TCD) ultrasound (2-MHz, Spencer Technologies, Seattle, WA, USA) was used to assess cerebral blood velocity (CBV), as an index of CBF, in the right MCA and left PCA. The TCD probes were attached to a specialized headband (model M600 bilateral head frame, Spencer Technologies), and each vessel was insonated through the trans-temporal window, using previously described location and standardization techniques (Willie *et al.*, 2011*a*).

Blood velocity and vessel diameter of the right CCA, ICA and ECA, and left VA, were measured using a 10-MHz multifrequency linear array duplex ultrasound (Terason uSmart 3300; Teratech, Burlington, MA, USA). Pulse-wave mode was used to measure peak blood velocity and arterial diameter was concurrently measured using B-mode imaging. The ICA and ECA

blood velocity and vessel diameter were measured ≥1.5 cm from the carotid bifurcation to avoid any turbulent or retrograde flow patterns, while VA blood velocity and diameter were measured between C4-C5 or C5-C6. The vessel location was decided on an individual basis to allow for reliable image acquisition, with the same location repeated within participants and between trials. Additionally, the insonation angle (60°) was unchanged throughout each test and, following acquisition of the first ultrasound image, there was no alteration of B-mode gain or dynamic range to avoid changes in arterial wall brightness/thickness.

Ultrasound recordings were captured and saved for offline analysis using custom edge-detection and wall tracking software (BloodFlow Analysis, version 5.1). This analysis method utilizes integration of diameter and velocity traces to calculate mean beat-to-beat flow at 30 Hz independent of observer bias (Woodman *et al.*, 2001). Mean shear rates were calculated as four times the peak velocity divided by vessel diameter (Woodman *et al.*, 2001). Mean blood flow was calculated as half of the time-averaged maximal velocity multiplied by the cross-sectional luminal area for a minimum of 12 cardiac cycles (Thomas *et al.*, 2015). The *g*CBF was estimated as twice the sum of the unilateral Q_{ICA} and Q_{VA} measurements. Lastly, cerebrovascular conductance (CVC) was calculated by dividing *g*CBF, ICA, ECA, VA, MCA, and PCA by MAP, respectively.

Neurovascular Coupling

The NVC test evoked selective changes in PCA*v* in response to activation of the visual cortex; whereas, the MCA*v* allowed for regional comparisons. Bilateral TCD ultrasound was used to measure left PCA*v* and right MCA*v*. Following two mins of rest, five cycles of repeated, alternating, 30s exposure to eyes-closed, and then eyes-open with a flashing checkerboard stimulus was completed, according to standardized guidelines (Phillips *et al.*, 2016). A previous study has evaluated the relationship between $CMRO_2$ and CBF during a flashing checkerboard visual stimulus using blood oxygen level dependent (BOLD) MRI in the visual cortex to validate this approach (Lin *et al.*, 2008). The researcher confirmed that the participant's eyes were closed and open during the respective trials. The PCA*v* and MCA*v* response to five cycles were exported on a breath-by-breath and beat-by-beat basis and used for data analysis (Phillips *et al.*, 2016). Here, for the time aligned NVC analysis, beat-to-beat (cardiovascular and cerebrovascular) and breath-by-breath (respiratory) data underwent cubic spline interpolation at

5 Hz using a custom built Matlab code (MathWorks, United States) (Phillips *et al.*, 2016). The NVC test provides insight into metabolic and myogenic regulation that is normalized to any temporal changes in arterial blood gases (Phillips *et al.*, 2016).

Thermometry

Esophageal temperature (T_{es}) was measured using a general purpose thermocouple (RET-1; Physitemp Instruments, Clifton, NJ, USA) inserted through the nasal passage and into the esophagus. The bottom of the esophageal thermistor probe was inserted to a depth calculated on an individual basis with the following formula: L (cm) = 0.228 x (standing height) – 0.194 (Mekjavić & Rempel, 1990). Rectal temperature (T_{re}) was also measured using a general purpose thermocouple (RET-1; Physitemp Instruments, Clifton, NJ, USA) inserted approximately 15-20 cm past the anal sphincter. The T_{es} was preferentially used as this method provides better temporal resolution due to the higher vascularization and superficial region of the esophagus; however, T_{re} was also measured to confirm that a steady-state temperature was achieved when participants experienced changes in respiration during the restoration of $P_{ET}CO_2$. The following results are presented as core temperature (Tc) (i.e., T_{es}; n=10 and T_{re}; n=1); one participant experienced transient reductions in temperature with excess cool air/ saliva passing over the esophageal thermocouple; however, all Tc methods were the same between conditions for each participant. Skin temperature (Tsk) was measured using skin thermistors (MLT422/A; ADInstruments, Colorado Springs, CO, USA) on the cheek (relevant for Q_{ECA}) and chest (as an index of changes in body Tsk). Thermal sensation and comfort were assessed at 10 mins intervals throughout EX and HS conditions using the ASHRAE thermal comfort scale. During the passive HS visit, participants were fitted with a full-body water-perfused suit (Med-Eng, Ottawa, ON, Canada) that covered the entire body except the hands, feet, and head. Throughout the PRE-HS assessment, thermoneutral 34°C water was circulated through the water-perfused suit; the water temperature was raised to 49°C for the passive heating protocol and blankets were used to accelerate the heating protocol as well as prevent heat loss and maintain Tc once the target had been reached.

Statistical Analyses

All data (apart from extracranial blood flow) were sampled continuously at 1000 Hz using an analogue-to-digital converter (Powerlab, 16/30; ADInstruments, Colorado Springs, CO, USA) and data were interfaced with LabChart (Version 7.1) and analyzed offline. All data are presented as mean ± SD unless otherwise stated. All CBF and NVC measures were conducted at rest (PRE) and repeated *during* temperature-matched EX and HS conditions. A linear mixed effects model with fixed effects of time (PRE vs. *during*) and condition (EX vs. HS) was used to compare all CBF variables (e.g., Q_{CCA}, Q_{ICA}, Q_{ECA}, Q_{VA}, MCA*v*, and PCA*v*). Subjects were included as a random effect and MAP was added as a co-variate for all CBF variables as MAP improved the model fit (-2 Log Likelihood). All NVC variables (PCA*v*, MCA*v*, PCA_{CVC}, MCA_{CVC}, MAP, $P_{ET}CO_2$) were compared as absolute peak response, *change* in absolute peak response from BL, time to peak response, average absolute response, average *change* in absolute response, relative peak response, and average relative response using the same linear mixed model described above. A Bonferroni correction was applied for multiple comparisons when significant interactions were detected. At least 30s averages were used for all CBF scans. Additionally, a 25s average during the eyes-closed stage was used to calculate relative percent change from BL for NVC. Absolute changes were calculated during the last 20s of visual activation stage of NVC (i.e., eyes-open). Statistical analyses were performed using SPSS software (IBM statistics, Version 22.0) and statistical significance was set at $P<0.05$.

RESULTS

Study participants' maximal achieved workload on a semi-recumbent cycle ergometer was 273±43 W with a respective VO_{2peak} of 43±7 $mL \cdot kg^{-1} \cdot min^{-1}$. During the submaximal exercise protocol, participants cycled at 50% workload max (i.e., 136±22 W); however, this value was lowered slightly (i.e., 99±23 W; 37±6% workload max) as participants reached their target peak Tc change (e.g., Δ0.75°C) after approximately 30-40 mins in an effort to stabilize Tc throughout NVC and CBF measures.

Thermometry

The change in Tc during submaximal cycling (*PRE-EX:* 37.32±0.38°C vs. *EX:* 38.07±0.38°C; Δ0.75±0.33°C) was well-matched during the passive HS trial (*PRE-HS:* 37.18±0.38°C vs. *HS:*

37.95±0.38°C; Δ0.77±0.33°C) (time effect: P<0.001; condition effect: P=0.074; interaction effect: P=0.855). Cheek Tsk was also increased during both EX (*PRE-EX:* 33.46±1.14°C vs. *EX:* 34.19±1.14°C; Δ0.73±1.30°C) and passive HS (*PRE-HS:* 33.39±1.14°C vs. *HS:* 35.00±1.14°C; Δ1.61±1.30°C) (time effect: P=0.003; condition effect: P=0.301; interaction effect: P=0.221). Chest Tsk was elevated during passive HS (*PRE-HS:* 34.46±0.90°C vs. *HS:* 37.38±0.95°C; Δ2.91±1.21°C; interaction: P<0.001) but not EX (*PRE-EX:* 33.42±0.90°C vs. *EX:* 33.95±0.90°C; Δ0.53±1.17°C; interaction: P=0.147). Perceived thermal sensation and comfort scores increased (i.e., hotter and greater discomfort) with prolonged duration of both EX and HS trials (time effect: both P<0.001); however, were not different between EX and HS conditions throughout each trial at respective durations of thermal stress (e.g., 10, 20, 30 mins; interaction effect: both P>0.05).

Ventilatory and hemodynamic (Table 1)

Throughout both EX and HS trials, $P_{ET}CO_2$ and $P_{ET}O_2$ were effectively maintained and, therefore, were not different between or within days (interaction effect: P=0.327 and P=0.952, respectively). Both EX and HS evoked increases in $\dot{V}_E$ (*EX:* Δ44.53±8.19 L·min^{-1}, P<0.001; and *HS:* Δ6.28±8.42 L·min^{-1}, P=0.019); however, $\dot{V}_E$ was higher during EX (P<0.001) with no between condition differences in *PRE-* intervention values (P=0.280) (see Table 1).

Overall, MAP was not significantly different throughout both EX and HS trials (Table 1; time effect: P=0.450); however, to account for intra-individual differences in MAP – as well as approximately 8±12 mmHg higher MAP during EX compared to HS (condition effect: P=0.064) – cerebrovascular conductance (CVC = flow or velocity/ MAP) was compared for all CBF variables (see *Cerebrovascular*). Both EX and HS evoked increases in cardiac output (CO) (*EX:* Δ7.2±1.7 L·min^{-1}, P<0.001; and *HS:* Δ1.7±1.7 L·min^{-1}, P=0.017) and HR (*EX:* Δ67±11 bpm, P<0.001; and *HS:* Δ27±10 bpm, P<0.001); however, CO and HR were higher during EX versus HS (both P<0.001) with no between condition differences in *PRE-* intervention values with either variable (both P>0.05). Overall, SV was higher throughout the EX versus HS trial (condition effect: P=0.029; interaction effect: P=0.270). Lastly, Q_{CCA} was increased to the same extent during both EX and HS (time effect: P=0.003; interaction effect: P=0.165).

Cerebrovascular (Table 2; Figure 1)

Overall, although Q_{ICA}, shear rate, and ICA_{CVC} were not significantly different between or within conditions (all P>0.05), Q_{ECA} was increased to the same extent during both conditions (*EX:* 42±58% vs. *HS:* 53±28%, respectively; time effect: P<0.001, interaction effect: P=0.618). Likewise, Q_{VA} showed comparable increases during both conditions (*EX:* 16±21% vs. *HS:* 16±23%, respectively; time effect: P=0.006, interaction effect: P=0.785). These results were unchanged when also presented as CVC (see Table 2). Both MCA*v* and PCA*v* increased during EX (*MCAv:* 17±13%, P=0.001; and *PCAv:* 13±9%, P=0.010); however, these variables were unchanged with HS (*MCAv:* -2±7%, P=0.747; and *PCAv:* -4±6%, P=0.560). Notably, MCA_{CVC} and PCA_{CVC} were not different between or within conditions (all P>0.05). The *g*CBF – driven by increases in Q_{VA} – was likewise elevated during both conditions (*EX:* 12±20% vs. *HS:* 14±14%, respectively; time effect: P=0.029, interaction effect: P=0.800) and this response was supported by *g*CVC (time effect: P=0.027; interaction effect: P=0.157).

Neurovascular Coupling (Table 3; Figure 2; Figure 3)

The absolute peak NVC response for PCA*v* was higher for EX versus HS conditions with no difference within trials (*PRE-EX:* 48.22±11.13 $cm \cdot s^{-1}$ vs. *EX:* 54.70±11.13 $cm \cdot s^{-1}$ and *PRE-HS:* 46.78±10.92 $cm \cdot s^{-1}$ vs. *HS:* 47.29±11.11 $cm \cdot s^{-1}$, respectively; time effect: P=0.064, condition effect: P=0.024, interaction effect: P=0.110). When expressed as PCA_{CVC}, this absolute peak NVC response was higher during both EX and HS versus PRE- testing with no differences between conditions (time effect: P=0.035; condition effect: P=0.471; interaction effect: P=0.180). The PCA*v* and PCA_{CVC} were elevated from PRE- values during both EX and HS (time effect: P=0.007 and P=0.029, respectively); whereas, when expressed as an absolute peak *change* from BL, this response was higher for the EX versus HS condition (*PRE-EX:* 9.35±2.98 $cm \cdot s^{-1}$ vs. *EX:* 9.02±2.98 $cm \cdot s^{-1}$ and *PRE-HS:* 8.06±2.88 $cm \cdot s^{-1}$ vs. *HS:* 7.20±2.97 $cm \cdot s^{-1}$, respectively; time effect: P=0.366, condition effect: P=0.025, interaction effect: P=0.685) with no difference within trials. This absolute peak *change* result was consistent between conditions when expressed as PCA_{CVC} (time effect: P=0.372; condition effect: P=0.035; interaction effect: P=0.418). The relative peak response for PCA*v* was reduced during both EX and HS versus PRE- values (*PRE-EX:* 24.35±5.69% vs. *EX:* 19.57±5.69% and *PRE-HS:* 20.89±5.45% vs. *HS:* 17.98±5.68%, respectively; time effect: P=0.014, condition effect: P=0.100, interaction effect: P=0.532), likely driven by the elevated PCA*v* evoked via EX. After accounting for MAP

changes, the relative peak response in PCA_{CVC} was higher for the EX versus HS condition (time effect: P=0.265; condition effect: P=0.021; interaction effect: P=0.849) with no difference within trials. Lastly, both the PCA*v* and PCA_{CVC} time to peak response was not different within or between conditions (all P>0.05).

DISCUSSION

The main findings of this study were: 1) Submaximal cycling exercise and temperature-matched passive heat stress, independent of changes in $P_{ET}CO_2$ and MAP, did not evoke increases in Q_{ICA}; 2) The Q_{ECA} was increased to the same extent with both temperature-matched exercise and passive heat stress; 3) The Q_{VA} and *g*CBF increased to the same extent during both exercise and temperature-matched passive heat stress; 4) Throughout both exercise and passive heat stress, the NVC response was preserved. These findings support our initial hypotheses of a temperature-dependent influence for selective increases in Q_{VA} and Q_{ECA} during exercise; such increases are independent of changes in $P_{ET}CO_2$ and MAP.

Cerebrovascular responses to submaximal exercise

The *g*CBF response during exercise is regulated via elevations in $PaCO_2$ and cerebral metabolism and is affected by contributions of systemic blood pressure and cerebrovascular tone (Ogoh & Ainslie, 2009). Recently, Smith and colleagues (2016) investigated the influence of $PaCO_2$ on cerebral vasodilation during recumbent submaximal exercise (i.e., <80% Wmax) and showed that increases in CBF were not different whether $P_{ET}CO_2$ increased with (poikilocapnia) or was kept constant at resting levels (isocapnia) (Smith *et al.*, 2016). Importantly, although *g*CBF was not influenced by $P_{ET}CO_2$ (Smith *et al.*, 2016), regional CBF increases in the posterior circulation have been reported during normal *poikilocapnic* submaximal exercise (e.g., 60-80% VO_{2peak} and 60% Wmax) with related elevations in $P_{ET}CO_2$ (Sato *et al.*, 2011); these data indicate that the regional – but not *g*CBF – is likely influenced by $PaCO_2$ (Sato *et al.*, 2011; Smith *et al.*, 2016). Additionally, throughout these submaximal exercise studies, the relative increases in Q_{VA} were reportedly higher (Sato *et al.*, 2011) or lower (Smith *et al.*, 2016) versus the Q_{ICA} response with poikilocapnia; however, these changes were reportedly not different during isocapnia (Smith *et al.*, 2016). These data are inconsistent with the current study where

the relative change in Q_{VA} was *higher* compared to Q_{ICA} during steady-state exercise at approximately 50% Wmax with isocapnia. An explanation for these between study differences may be related to the duration of exercise (e.g., 60 mins in the present study versus 5-mins steady-state progressive exercise intensity in Sato *et al.*, 2011 and Smith *et al.*, 2016) and posture (e.g., semi-recumbent in the present study and Sato *et al.*, 2011 versus recumbent in Smith *et al.*, 2016) (Ota *et al.*, 2019). Although HR, $\dot{V}_E$, $P_{ET}CO_2$, and $P_{ET}O_2$ were comparable between the current study and Smith and colleagues (2016), during related exercise intensity (i.e., <60% Wmax), MAP was appreciably lower (approximately 94 mmHg vs. 105 mmHg) which may contribute to higher CVC during exercise in the present study. Although resting MAP was not different between the current study and Smith and colleagues (2016), resting HR was lower in the present study (approximately 67 bpm vs. 74 bpm) and Wmax was appreciably higher (approximately 275 W vs. 200 W); therefore, differences in fitness and/or body posture (e.g., semi-recumbent vs. supine) may explain the lower MAP response during exercise, thereby influencing CVC regulation in the current study.

Sato and colleagues (2016) have recently reported that increases in Q_{ICA} throughout 40 mins of semi-recumbent cycling at 60% VO_{2peak} with varying degrees of hyperthermia (e.g., +1.2-1.6°C Tc) is related to the increases in $P_{ET}CO_2$ (Sato *et al.*, 2016). This finding supports the current study whereby Q_{ICA} was unchanged throughout exercise when $P_{ET}CO_2$ was maintained, and also relates to previous work indicating an integral role of CO_2 in mediating CBF during passive heat stress (Bain *et al.*, 2013). Both Sato and colleagues (2011) and Smith and coworkers (2016) have reported greater elevations in posterior CBF (e.g., Q_{VA} and PCA*v*, respectively) with progressive increases in cycling exercise intensity (semi-recumbent and supine, respectively) under poikilocapnic conditions (Sato *et al.*, 2011; Smith *et al.*, 2016). As such, these data support the possibility of a higher cerebrovascular CO_2 reactivity in the posterior circulation as previously reported at rest (Willie *et al.*, 2012). Conversely, in the current study, Q_{VA} was increased to the same extent during both exercise and passive heat stress under *isocapnic* conditions with no change in Q_{ICA}; therefore, as discussed next, it seems possible that there is a temperature-mediated control of regional CBF in the posterior circulation during submaximal steady-state cycling exercise.

Why are there selective increases in posterior CBF during exercise?

The selective increase in $\dot{Q}_{VA}$ and, therefore, overall increase in *g*CBF observed in the present study, is likely related to compensatory increases in cerebral metabolism (Fisher *et al.*, 2013). As NVC describes coupling of CBF to local increases in neural activity and metabolism, and this response was preserved during submaximal exercise, the observed increases in PCA*v* provoked with exercise indicate appropriately matched CBF to elevated $CMRO_2$ in the posterior circulation. Related to the current study, NVC has been reportedly maintained with upright cycling exercise at 60% of VO_{2max} during *poikilocapnia*, with comparable absolute peak change in PCA*v* (i.e., both approximately 9 $cm \cdot s^{-1}$) (Willie *et al.*, 2011*b*). This NVC response involves localized increases in intracellular Ca^{2+}, NO, and ATP; therefore, contributing to retrograde propagation of vasodilatory signals to elicit increases in CBF [reviewed in: (Iadecola, 2017)]. Previously, Yamaguchi and colleagues (2015) have reported an attenuated contribution of MAP on NVC with high-intensity exercise (Yamaguchi *et al.*, 2015*b*), and that exhaustive exercise attenuates NVC by blunting the exercise pressor reflex to visual stimulation (Yamaguchi *et al.*, 2015*a*). These latter results are likely explained by exercise-induced hyperventilation and related hypocapnia with poikilocapnic high-intensity exercise. Indeed, hypocapnia-evoked cerebral vasoconstriction reportedly reduces NVC at rest (Szabo *et al.*, 2011). Additionally, this uncoupling of the NVC response at maximal exercise is further supported by increases in $CMRO_2$ in parallel with reductions in CBF [reviewed in: (Smith & Ainslie, 2017)]. Further, as discussed next, the influence of hotter inflow CBF on cerebral tissue temperature, and therefore, cerebral metabolism may provide further insight into the elevation in $CMRO_2$ achieved with exercise (Ide & Secher, 2000; Fisher *et al.*, 2013; Smith *et al.*, 2014).

Core temperature-mediated CBF regulation

Changes in Tc can have a large effect on $CMRO_2$, such that the change in biological activity for a given change in temperature can be expressed as a Q_{10} temperature coefficient [reviewed in: (Bain *et al.*, 2015)]. Values derived with anesthesia and hypothermia (Donnelly *et al.*, 1956; MacVeigh *et al.*, 1997) indicate that human cerebral tissue corresponds to a Q_{10} of approximately 2-3, i.e., $CMRO_2$ decreases by approximately 10-20% per degree Celsius reduction in cerebral temperature. Assuming a Q_{10} of approximately two (Donnelly *et al.*, 1956; MacVeigh *et al.*, 1997; Nybo *et al.*, 2002), the +0.75°C increase in Tc in the present study would indicate approximately 7.5% increase in $CMRO_2$ during passive heat stress; however, regional

differences in cerebral temperature (Olszewski 1952) and metabolism (Qian *et al.*, 2014) may have also contributed to the current selective CBF regulation. Increases in $CMRO_2$ may mediate selective increases in Q_{VA} as the brainstem and hypothalamic thermoregulatory centers sensitive to changes in Tc are supplied by the posterior cerebral circulation (Siemens & Kamm, 2018). Additionally, as the NVC response to passive heat stress was preserved in the present study, these data indicate sufficiently matched CBF to local $CMRO_2$ (Yablonskiy *et al.*, 2000), likely provoked by higher regional cerebral tissue temperature (i.e., Q_{10} effect; +0.75°C Tc) (Nunneley *et al.*, 2002) and perhaps reflective of increases in Q_{VA} with heat stress.

Findings from the current study indicate changes in Tc may account for up to approximately 75% of the increases in Q_{ECA} during submaximal cycling exercise (e.g., relative increase in Q_{ECA} during EX: 42±58% vs. HS: 53±28%). Further, passive heat stress (i.e., +1.5°C Tc) reportedly provokes 23% increases in systemic metabolism and corresponding regional elevations in $CMRO_2$ in the lateral cerebellum (Nunneley *et al.*, 2002), perhaps indicating thermoregulatory sensitivity in the posterior cerebrovasculature. Regional increases in CBF (via PET imaging) have also been recently reported in the brainstem and cerebellum during submaximal (i.e., 30% HR reserve) supine cycling exercise, indicating reflex cardiovascular control of CBF distribution during exercise (Hiura *et al.*, 2018). Additionally, Sato and colleagues (2016) reported that CVC in the ICA was significantly reduced at 40 mins during hyperthermic exercise, whereas, it was preserved in the VA (Sato *et al.*, 2016). These results indicate that temperature and/or related increases in $CMRO_2$ – and not $PaCO_2$ or MAP – *per se* may regulate regional CBF during submaximal exercise as posterior CBF was favoured during *poikilocapnia* (Sato *et al.*, 2016) as well as *isocapnia* (per current findings; Fig. 1).

Perspectives

Findings from the current study indicate that the therapeutic cerebrovascular effects of exercise (e.g., increases in regional CBF) may be achieved with moderate-level passive heat stress; as such, these findings may provide support for passive heat stress as a novel exercise alternative for clinical populations with impaired cerebrovascular health and/or inability to participate in aerobic exercise (e.g., spinal cord injury, cerebral palsy, multiple sclerosis) (Phillips *et al.*, 2017; Metzger *et al.*, 2018; Coombs *et al.*, 2019); however, future research on exercise in the heat is required for these clinical groups. Favourable blood flow patterns (e.g., antegrade shear stress)

evoked via exercise and passive heat stress can acutely (Carter *et al.*, 2013) and chronically (Carter *et al.*, 2014) improve endothelial function (Brunt *et al.*, 2016; 2018). Indeed, *in vitro* evidence suggests an increased nitric oxide (NO) bioavailability in cerebral artery cells exposed to shear stress (Mashour & Boock, 1999), thus indicating an endothelium dependent shear-mediated regulation of CBF. As hyperventilatory-induced hypocapnia occurs at approximately +0.5-1.0°C (Fan *et al.*, 2008; Tsuji *et al.*, 2017), targeted cerebrovascular heat therapy would likely be slightly less than the present level of passive heat stress achieved in this study (e.g., +0.75°C) to maximize increases in CBF in a practical setting. Additionally, typical Finnish sauna bathing can acutely increase Tc by up to +2.0°C (Laukkanen *et al.*, 2018) and the incidence of cerebrovascular diseases is lower in those who frequently participate in sauna bathing (Kunutsor *et al.*, 2018); therefore, further investigations with both acute and chronic heating interventions are required to prescribe the ideal level of heat therapy for both systemic and cerebrovascular improvements. Lastly, results from the present study suggest that changes in Tc should be considered when assessing CBF regulation during exercise to provide context for comparisons between different exercise intensities and durations.

Passive heat stress (+1.5°C Tc) reportedly increases systemic metabolism by approximately 23% and provokes related regional increases in $CMRO_2$ in the hypothalamus, thalamus, corpus callosum, cingulate gyrus, and cerebellum (Nunneley *et al.*, 2002). The preoptic-anterior hypothalamus – supplied in part by posterior aspects of the Circle of Willis – plays an important role in body temperature regulation and fever (Boulant, 2000) via efferent pathways regulating cutaneous blood flow and sweating (McAllen & McKinley, 2018). Additionally, temperature-dependent increases in metabolic flux can increase skeletal muscle oxidative stress via cellular respiration (Jarmuszkiewicz *et al.*, 2015) that may exacerbate the heat-evoked pro-inflammatory response (Bouchama & Knochel, 2002). Local CBF supplying the hypothalamus is reportedly preserved during anesthesia and across wide ranges of MAP (e.g., 41-140 mmHg) in rabbits (Cranston & Rosendorff, 1971); therefore, temperature sensitivity in this region likely plays a large role in CBF regulation. Lastly, selective increases in posterior CBF during submaximal cycling exercise may improve blood flow regulation supplying the brainstem (Hiura *et al.*, 2018). Such increases in regional CBF supplying the brainstem, cerebellum, and hypothalamus were reportedly consistent with the exercise-induced elevations in

MAP (Hiura *et al.*, 2018); as such, regional CBF distribution may support improved reflex cardiovascular control (e.g., autonomic regulation of MAP and HR responses) during exercise.

Experimental limitations

The present study utilized dynamic end-tidal control to effectively clamp $P_{ET}CO_2$ and $P_{ET}O_2$ throughout exercise and passive heat stress to their respective resting values. This system regulates end-tidal gases on a breath-by-breath basis by providing individualized inspired gas mixtures of CO_2, O_2, and N_2, independent of ventilation (Tymko *et al.*, 2015; 2016). Importantly, this method provides accurate $P_{ET}CO_2$ control as a surrogate for $PaCO_2$ as the gradient between $P_{ET}CO_2$ and $PaCO_2$ is approximately 1 mmHg (Tymko *et al.*, 2015). Brothers and colleagues (2011) have reported that $P_{ET}CO_2$ accurately reflects $PaCO_2$ during passive heat stress of approximately 1.0-1.5°C; therefore, effective end-tidal clamping in the present study was likely adequate to control $PaCO_2$ (Brothers *et al.*, 2011). With progressive increases in exercise intensity, $PaCO_2$ is reduced, such that the end-tidal to arterial CO_2 gradient increases; as such, $P_{ET}CO_2$ values typically overestimate $PaCO_2$ (Liu *et al.*, 1995). Briefly, $P_{ET}CO_2$ reportedly *underestimates* $PaCO_2$ slightly at rest (Robbins *et al.*, 1990) and *overestimates* $PaCO_2$ during exercise (Jones *et al.*, 1979; Robbins *et al.*, 1990). As a result, controlling $P_{ET}CO_2$ values without direct $PaCO_2$ and/or blood temperature correction may have overestimated arterial PCO_2 by approximately 1-2 mmHg throughout the exercise trial in the current study (Reyna *et al.*, 2015). We feel, however, that this possible error will not have an appreciable influence on our main outcome variables. Lastly, although we are not aware of any evidence of sex-related differences in NVC (Phillips *et al.*, 2016), we do not know if there are sex differences in cerebrovascular and/or temperature regulation during exercise and passive heat stress; as such, our results are mostly applicable to young males.

Technical considerations

Assessment of CBV via transcranial Doppler (TCD) ultrasound is an adequate surrogate of absolute CBF only if the insonated cerebral vessel diameter does not change (Ainslie & Hoiland, 2014). Importantly, *in vivo* evidence supports small but significant cerebral vasoconstriction (i.e., reduced diameter) in the MCA with exercise-induced sympathetic activation (Verbree *et al.*, 2017); as such, conceivable reductions in MCA diameter, paired with the observed increase in

MCA*v*, may explain the unchanged Q_{ICA} seen during exercise. Additionally, the ICA supplies both the anterior cerebral artery (ACA) and MCA; therefore, the assumption of unity between Q_{ICA} and MCA flow/ velocity is contingent on the consistent distributive relationship between the MCA and ACA [discussed in: (Hoiland & Ainslie, 2016)]. Likewise, the vertebro-basilar circulation is highly anatomically complex; that is, the VA supplies extracranial branches of the deep cervical artery and inferior thyroid artery, as well as anterior and posterior spinal arteries, perforating branches to the medulla, and the posterior inferior cerebellar artery before feeding the basilar artery and PCA. The inconsistency between increases in Q_{VA} and unchanged PCA*v* during passive heat stress may be explained by redistribution of Q_{VA} to intracerebral arteries supplying the brainstem and cerebellum due to higher thermoregulatory sensitivity in these regions (Nunneley *et al.*, 2002).

CONCLUSION

In conclusion, independent of changes in $P_{ET}CO_2$ and MAP, our findings support our initial hypotheses of a temperature-dependent influence of selective increases in Q_{VA} and Q_{ECA} during exercise. The detailed mechanism(s) (i.e., Q_{10} effect and/or metabolism) and clinical implications of these findings remains to be explored.

Competing interests

None to declare.

Author contributions

This study was performed at the University of British Columbia Okanagan in Kelowna, BC, Canada. HGC, PNA, and SJEL conceived and designed the research. HGC, GBC, CAH, RLH, and AP acquired the data. HGC analyzed the data. HGC, PNA, and SJEL interpreted the data. All authors revised the manuscript and provided intellectual feedback and agree to be accountable for all aspects of the work.

Funding

This study was funded by the Natural Sciences and Engineering Research Council of Canada (PNA) and a Canada Research Chair (PNA). HGC was supported by a NSERC CGS-Master's Scholarship.

Acknowledgements

We appreciate the time and effort spent by our volunteer participants in the present study.

552 REFERENCES

553

554 Ainslie PN & Hoiland RL (2014). Transcranial Doppler ultrasound: Valid, invalid, or both?
555 *Journal of Applied Physiology* **117,** 1081–1083.

556 Bain AR, Hoiland RL, Donnelly J, Nowak-Flück D, Sekhon M, Tymko MM, Greiner JJ,
557 DeSouza CA, Ainslie PN (2019). Cerebral metabolism, oxidation, and inflammation in
558 severe passive hyperthermia with and without respiratory alkalosis. *J Physiol* in review.
559

560 Bain AR, Nybo L & Ainslie PN (2015). Cerebral Vascular Control and Metabolism in Heat
561 Stress. *Compr Physiol* **5,** 1345–1380.

562 Bain AR, Smith KJ, Lewis NC, Foster GE, Wildfong KW, Willie CK, Hartley GL, Cheung SS &
563 Ainslie PN (2013). Regional changes in brain blood flow during severe passive
564 hyperthermia: effects of PaCO2 and extracranial blood flow. *J Appl Physiol* **115,** 653–659.

565 Bouchama A & Knochel JP (2002). Heat stroke. *N Engl J Med* **346,** 1978–1988.

566 Boulant JA (2000). Role of the preoptic-anterior hypothalamus in thermoregulation and fever.
567 *Clin Infect Dis* **31 Suppl 5,** S157–S161.

568 Brothers RM, Ganio MS, Hubing KA, Hastings JL & Crandall CG (2011). End-tidal carbon
569 dioxide tension reflects arterial carbon dioxide tension in the heat-stressed human with and
570 without simulated hemorrhage. *Am J Physiol Regul Integr Comp Physiol* **300,** R978–R983.

571 Brothers RM, Wingo JE, Hubing KA & Crandall CG (2009). The effects of reduced end-tidal
572 carbon dioxide tension on cerebral blood flow during heat stress. *J Physiol (Lond)* **587,**
573 3921–3927.

574 Brunt VE, Howard MJ, Francisco MA, Ely BR & Minson CT (2016). Passive heat therapy
575 improves endothelial function, arterial stiffness and blood pressure in sedentary humans. *J*
576 *Physiol (Lond)* **594,** 5329–5342.

577 Brunt VE, Wiedenfeld-Needham K, Comrada LN & Minson CT (2018). Passive heat therapy
578 protects against endothelial cell hypoxia-reoxygenation via effects of elevations in
579 temperature and circulating factors. *J Physiol (Lond)* **596,** 4831–4845.

580 Carter HH, Dawson EA, Birk GK, Spence AL, Naylor LH, Cable NT, Thijssen DHJ & Green DJ
581 (2013). Effect of SR manipulation on conduit artery dilation in humans. *Hypertension* **61,**
582 143–150.

583 Carter HH, Spence AL, Atkinson CL, Pugh CJA, Naylor LH & Green DJ (2014). Repeated core
584 temperature elevation induces conduit artery adaptation in humans. *Eur J Appl Physiol* **114,**
585 859–865.

586 Coombs GB, Vucina D, Caldwell HG, Barak OF, Mijacika T, Lee AHX, Sarafis ZK, Squair JW,
587 Krassioukov AV, Phillips AA, Dujic Z & Ainslie PN (2019). Cerebrovascular function is
588 preserved during mild hyperthermia in cervical spinal cord injury. *Spinal Cord* **81,** 723–726.

589 Crandall CG & González-Alonso J (2010). Cardiovascular function in the heat-stressed human.
590 *Acta Physiol (Oxf)* **199,** 407–423.

591 Crandall CG, Etzel RA & Farr DB (1999). Cardiopulmonary baroreceptor control of muscle
592 sympathetic nerve activity in heat-stressed humans. *American Journal of Physiology-Legacy*
593 *Content* **277,** H2348–H2352.

594 Cranston WI & Rosendorff C (1971). Local blood flow, cerebrovascular autoregulation and CO2
595 responsiveness in the rabbit hypothalamus. *J Physiol (Lond)* **215,** 577–590.

596 Donnelly C, Frobese AS, MACKRELL TN, STONE HH & TRUTER MR (1956). The effect of
597 lowered body temperature on the cerebral hemodynamics and metabolism of man. *Surg*
598 *Forum* **6,** 129–134.

599 Fan J-L, Cotter JD, Lucas RAI, Thomas K, Wilson L & Ainslie PN (2008). Human
600 cardiorespiratory and cerebrovascular function during severe passive hyperthermia: effects
601 of mild hypohydration. *J Appl Physiol* **105,** 433–445.

602 Fisher JP, Hartwich D, Seifert T, Olesen ND, McNulty CL, Nielsen HB, van Lieshout JJ &
603 Secher NH (2013). Cerebral perfusion, oxygenation and metabolism during exercise in
604 young and elderly individuals. *J Physiol (Lond)* **591,** 1859–1870.

605 Fujii N, Tsuji B, Honda Y, Kondo N & Nishiyasu T (2015). Effect of short-term exercise-heat
606 acclimation on ventilatory and cerebral blood flow responses to passive heating at rest in
607 humans. *J Appl Physiol* **119,** 435–444.

608 Gupte AA, Bomhoff GL, Touchberry CD & Geiger PC (2011). Acute heat treatment improves
609 insulin-stimulated glucose uptake in aged skeletal muscle. *J Appl Physiol* **110,** 451–457.

610 Hiura M, Nariai T, Sakata M, Muta A, Ishibashi K, Wagatsuma K, Tago T, Toyohara J, Ishii K
611 & Maehara T (2018). Response of Cerebral Blood Flow and Blood Pressure to Dynamic
612 Exercise: A Study Using PET. *Int J Sports Med* **39,** 181–188.

613 Hoiland RL & Ainslie PN (2016). CrossTalk proposal: The middle cerebral artery diameter does
614 change during alterations in arterial blood gases and blood pressure. *J Physiol (Lond)* **594,**
615 4073–4075.

616 Iadecola C (2017). The Neurovascular Unit Coming of Age: A Journey through Neurovascular
617 Coupling in Health and Disease. *Neuron* **96,** 17–42.

618 Ide K & Secher NH (2000). Cerebral blood flow and metabolism during exercise. *Progress in*
619 *Neurobiology* **61,** 397–414.

Jarmuszkiewicz W, Woyda-Ploszczyca A, Koziel A, Majerczak J & Zoladz JA (2015). Temperature controls oxidative phosphorylation and reactive oxygen species production through uncoupling in rat skeletal muscle mitochondria. *Free Radic Biol Med* **83,** 12–20.

Jones NL, Robertson DG & Kane JW (1979). Difference between end-tidal and arterial PCO2 in exercise. *J Appl Physiol Respir Environ Exerc Physiol* **47,** 954–960.

Kunutsor SK, Khan H, Zaccardi F, Laukkanen T, Willeit P & Laukkanen JA (2018). Sauna bathing reduces the risk of stroke in Finnish men and women: A prospective cohort study. *Neurology* **90,** e1937–e1944.

Larsen TS, Rasmussen P, Overgaard M, Secher NH & Nielsen HB (2008). Non-selective β-adrenergic blockade prevents reduction of the cerebral metabolic ratio during exhaustive exercise in humans. *J Physiol (Lond)* **586,** 2807–2815.

Laukkanen T, Kunutsor SK, Zaccardi F, Lee E, Willeit P, Khan H & Laukkanen JA (2018). Acute effects of sauna bathing on cardiovascular function. *J Hum Hypertens* **32,** 129–138.

Lin A-L, Fox PT, Yang Y, Lu H, Tan L-H & Gao J-H (2008). Evaluation of MRI models in the measurement of CMRO2 and its relationship with CBF. *Magnetic Resonance in Medicine* **60,** 380–389.

Liu Z, Vargas F, Stansbury D, Sasse SA & Light RW (1995). Comparison of the end-tidal arterial PCO2 gradient during exercise in normal subjects and in patients with severe COPD. *Chest* **107,** 1218–1224.

MacVeigh I, Cook DJ, Orszulak TA, Daly RC & Munnikhuysen DE (1997). Nitrous oxide method of measuring cerebral blood flow during hypothermic cardiopulmonary bypass. *Ann Thorac Surg* **63,** 736–740.

Mashour GA & Boock RJ (1999). Effects of shear stress on nitric oxide levels of human cerebral endothelial cells cultured in an artificial capillary system. *Brain Res* **842,** 233–238.

McAllen RM & McKinley MJ (2018). Efferent thermoregulatory pathways regulating cutaneous blood flow and sweating. *Handb Clin Neurol* **156,** 305–316.

Mekjavić IB & Rempel ME (1990). Determination of esophageal probe insertion length based on standing and sitting height. *Journal of Applied Physiology* **69,** 376–379.

Metzger A, Le Bars E, Deverdun J, Molino F, Maréchal B, Picot M-C, Ayrignac X, Carra C, Bauchet L, Krainik A, Labauge P & Menjot de Champfleur N (2018). Is impaired cerebral vasoreactivity an early marker of cognitive decline in multiple sclerosis patients? *Eur Radiol* **28,** 1204–1214.

Miyamoto H, Kai H, Nakaura H, Osada K, Mizuta Y, Matsumoto A & Imaizumi T (2005). Safety and efficacy of repeated sauna bathing in patients with chronic systolic heart failure: a preliminary report. *J Card Fail* **11,** 432–436.

655 Nelson MD, Haykowsky MJ, Stickland MK, Altamirano-Diaz LA, Willie CK, Smith KJ,
656 Petersen SR & Ainslie PN (2011). Reductions in cerebral blood flow during passive heat
657 stress in humans: partitioning the mechanisms. *J Physiol (Lond)* **589,** 4053–4064.

658 Nunneley SA, Martin CC, Slauson JW, Hearon CM, Nickerson LDH & Mason PA (2002).
659 Changes in regional cerebral metabolism during systemic hyperthermia in humans. *Journal*
660 *of Applied Physiology* **92,** 846–851.

661 Nybo L, Møller K, Volianitis S, Nielsen B & Secher NH (2002). Effects of hyperthermia on
662 cerebral blood flow and metabolism during prolonged exercise in humans. *Journal of*
663 *Applied Physiology* **93,** 58–64.

664 Ogoh S & Ainslie PN (2009). Regulatory mechanisms of cerebral blood flow during exercise:
665 new concepts. *Exerc Sport Sci Rev* **37,** 123–129.

666 Ogoh S, Sato K, Okazaki K, Miyamoto T, Hirasawa A & Shibasaki M (2014). Hyperthermia
667 modulates regional differences in cerebral blood flow to changes in CO2. *J Appl Physiol*
668 **117,** 46–52.

669 Ogoh S, Sato K, Okazaki K, Miyamoto T, Hirasawa A, Morimoto K & Shibasaki M (2013).
670 Blood Flow Distribution during Heat Stress: Cerebral and Systemic Blood Flow. *Journal of*
671 *Cerebral Blood Flow & Metabolism* **33,** 1915–1920.

672 Ota A, Takeda R, Imai D, Naghavi N, Kawai E, Saho K, Morita E, Suzuki Y, Yokoyama H,
673 Miyagawa T & Okazaki K (2019). The effects of aging on the distribution of cerebral blood
674 flow with postural changes and mild hyperthermia. *Eur J Appl Physiol* **119,** 1261–1272.

675 Périard JD, Travers GJS, Racinais S & Sawka MN (2016). Cardiovascular adaptations
676 supporting human exercise-heat acclimation. *Auton Neurosci* **196,** 52–62.

677 Phillips AA, Chan FH, Zheng MMZ, Krassioukov AV & Ainslie PN (2016). Neurovascular
678 coupling in humans: Physiology, methodological advances and clinical implications. *J Cereb*
679 *Blood Flow Metab* **36,** 647–664.

680 Phillips AA, Squair JR, Currie KD, Tzeng YC, Ainslie PN & Krassioukov AV (2017). 2015
681 ParaPan American Games: Autonomic Function, But Not Physical Activity, Is Associated
682 with Vascular-Cognitive Impairment in Spinal Cord Injury. *J Neurotrauma* **34,** 1283–1288.

683 Qian S, Jiang Q, Liu K, Li B, Li M, Li L, Yang X, Yang Z & Sun G (2014). Effects of short-term
684 environmental hyperthermia on patterns of cerebral blood flow. *Physiol Behav* **128,** 99–107.

685 Reyna, J.L. et al., 2015. Arterial to end-tidal PCO2 difference during exercise in normoxia and
686 severe acute hypoxia: importance of blood temperature correction. *Wiley Online Library*.

687 Robbins PA, Conway J, Cunningham DA, Khamnei S & Paterson DJ (1990). A comparison of
688 indirect methods for continuous estimation of arterial PCO2 in men. *Journal of Applied*
689 *Physiology* **68,** 1727–1731.

690 Sato K, Ogoh S, Hirasawa A, Oue A & Sadamoto T (2011). The distribution of blood flow in the
691 carotid and vertebral arteries during dynamic exercise in humans. *J Physiol (Lond)* **589,**
692 2847–2856.

693 Sato K, Oue A, Yoneya M, Sadamoto T & Ogoh S (2016). Heat stress redistributes blood flow in
694 arteries of the brain during dynamic exercise. *J Appl Physiol* **120,** 766–773.

695 Siemens J & Kamm GB (2018). Cellular populations and thermosensing mechanisms of the
696 hypothalamic thermoregulatory center. *Pflugers Arch* **470,** 809–822.

697 Smith KJ & Ainslie PN (2017). Regulation of cerebral blood flow and metabolism during
698 exercise. *Exp Physiol*; DOI: 10.1113/EP086249.

699 Smith KJ, MacLeod D, Willie CK, Lewis NCS, Hoiland RL, Ikeda K, Tymko MM, Donnelly J,
700 Day TA, MacLeod N, Lucas SJE & Ainslie PN (2014). Influence of high altitude on cerebral
701 blood flow and fuel utilization during exercise and recovery. *J Physiol (Lond)* **592,** 5507–
702 5527.

703 Smith KJ, Wildfong KW, Hoiland RL, Harper M, Lewis NC, Pool A, Smith SL, Kuca T, Foster
704 GE & Ainslie PN (2016). Role of CO2 in the cerebral hyperemic response to incremental
705 normoxic and hyperoxic exercise. *J Appl Physiol* **120,** 843–854.

706 Szabo K, Lako E, Juhasz T, Rosengarten B, Csiba L & Olah L (2011). Hypocapnia induced
707 vasoconstriction significantly inhibits the neurovascular coupling in humans. *J Neurol Sci*
708 **309,** 58–62.

709 Thomas KN, Lewis NCS, Hill BG & Ainslie PN (2015). Technical recommendations for the use
710 of carotid duplex ultrasound for the assessment of extracranial blood flow. *Am J Physiol*
711 *Regul Integr Comp Physiol* **309,** 1–7.

712 Tsuji B, Filingeri D, Honda Y, Eguchi T, Fujii N, Kondo N & Nishiyasu T (2017). Effect of
713 hypocapnia on the sensitivity of hyperthermic hyperventilation and the cerebrovascular
714 response in resting heated humans. *J Appl Physiol*jap.00232.2017.

715 Tsuji B, Hoshi Y, Honda Y, Fujii N, Sasaki Y, Cheung SS, Kondo N & Nishiyasu T (2019).
716 Respiratory mechanics and cerebral blood flow during heat-induced hyperventilation and its
717 voluntary suppression in passively heated humans. *Physiol Rep* **7,** e13967.

718 Tymko MM, Ainslie PN, Macleod DB, Willie CK & Foster GE (2015). End tidal-to-arterial CO
719 2and O 2gas gradients at low- and high-altitude during dynamic end-tidal forcing. *Am J*
720 *Physiol Regul Integr Comp Physiol* **308,** R895–R906.

721 Tymko MM, Hoiland RL, Kuca T, Boulet LM, Tremblay JC, Pinske BK, Williams AM & Foster
722 GE (2016). Measuring the human ventilatory and cerebral blood flow response to CO2: a
723 technical consideration for the end-tidal-to-arterial gas gradient. *J Appl Physiol* **120,** 282–
724 296.

725 Verbree J, Bronzwaer A, van Buchem MA, Daemen M, van Lieshout JJ & van Osch M (2017).
726 Middle cerebral artery diameter changes during rhythmic handgrip exercise in humans. *J*
727 *Cereb Blood Flow Metab* **37,** 2921–2927.

728 Willie CK & Ainslie PN (2011). Cool head, hot brain: cerebral blood flow distribution during
729 exercise. *J Physiol (Lond)* **589,** 2657–2658.

730 Willie CK, Colino FL, Bailey DM, Tzeng YC, Binsted G, Jones LW, Haykowsky MJ, Bellapart
731 J, Ogoh S, Smith KJ, Smirl JD, Day TA, Lucas SJ, Eller LK & Ainslie PN (2011*a*). Utility
732 of transcranial Doppler ultrasound for the integrative assessment of cerebrovascular
733 function. *J Neurosci Methods* **196,** 221–237.

734 Willie CK, Cowan EC, Ainslie PN, Taylor CE, Smith KJ, Sin PYW & Tzeng YC (2011*b*).
735 Neurovascular coupling and distribution of cerebral blood flow during exercise. *J Neurosci*
736 *Methods* **198,** 270–273.

737 Willie CK, Macleod DB, Shaw AD, Smith KJ, Tzeng YC, Eves ND, Ikeda K, Graham J, Lewis
738 NC, Day TA & Ainslie PN (2012). Regional brain blood flow in man during acute changes
739 in arterial blood gases. *J Physiol (Lond)* **590,** 3261–3275.

740 Wilson TE, Cui J & Crandall CG (2002). Effect of whole-body and local heating on cutaneous
741 vasoconstrictor responses in humans. *Auton Neurosci* **97,** 122–128.

742 Woodman RJ, Playford DA, Watts GF, Cheetham C, Reed C, Taylor RR, Puddey IB, Beilin LJ,
743 Burke V, Mori TA & Green D (2001). Improved analysis of brachial artery ultrasound using
744 a novel edge-detection software system. *Journal of Applied Physiology* **91,** 929–937.

745 Yablonskiy DA, Ackerman JJH & Raichle ME (2000). Coupling between changes in human
746 brain temperature and oxidative metabolism during prolonged visual stimulation.
747 *Proceedings of the National Academy of Sciences* **97,** 7603–7608.

748 Yamaguchi Y, Ikemura T & Hayashi N (2015*a*). Exhaustive exercise attenuates the
749 neurovascular coupling by blunting the pressor response to visual stimulation. *Biomed Res*
750 *Int* **2015,** 671063–671066.

751 Yamaguchi Y, Ikemura T, Kashima H & Hayashi N (2015*b*). Effects of vasodilatation and
752 pressor response on neurovascular coupling during dynamic exercise. *Eur J Appl Physiol*
753 **115,** 619–625.

Table 1. Absolute ventilatory and hemodynamic parameters at rest (PRE) and during submaximal exercise (EX) and passive heat stress (HS)

	PRE-EX	EX	PRE-HS	HS	*P-Values*		
Ventilatory					*Time*	*Condition*	*Time*Condition*
$P_{ET}CO_2$ (mmHg)	40.9±3.7	42.0±4.2	41.0±3.5	41.2±3.6	P=0.089	P=0.482	P=0.327
$P_{ET}O_2$ (mmHg)	90.7±4.5	89.5±4.2	91.3±4.8	90.0±5.0	P=0.217	P=0.585	P=0.952
$\dot{V}_E$ (L·min^{-1})	14.9±4.4$^{\$}$	59.5±10.2$^{\#\$}$	12.2±3.4$^{\%}$	18.4±5.6$^{\#\%}$	**P<0.001**	**P<0.001**	**P<0.001**
V_T (L)	1.2±0.2$^{\$}$	2.7±0.7$^{\#\$}$	1.0±0.4	1.4±0.6$^{\#}$	**P<0.001**	**P<0.001**	**P<0.001**
RR (BPM)	13±5$^{\$}$	23±4$^{\#\$}$	13±4	15±5$^{\#}$	**P<0.001**	**P<0.001**	**P<0.001**
Hemodynamic							
MAP (mmHg)	90±9	95±8	88±11	87±11	P=0.450	P=0.064	P=0.184
SBP (mmHg)	122±7	131±7	120±13	122±14	P=0.105	P=0.066	P=0.245
DBP (mmHg)	72±10	74±9	71±11^{+}	66±10^{+}	P=0.369	**P=0.036**	P=0.106
CO (L·min^{-1})	7.3±1.5$^{\$}$	14.5±1.7$^{\#\$}$	6.3±1.5$^{\%}$	8.0±1.1$^{\#\%}$	**P<0.001**	**P<0.001**	**P<0.001**
HR (bpm)	69±16$^{\$}$	136±13$^{\#\$}$	65±13$^{\%}$	92±23$^{\#\%}$	**P<0.001**	**P<0.001**	**P<0.001**
SV (mL)	105.8±11.5	107.5±17.8	100.3±11.8^{+}	92.0±24.0^{+}	P=0.467	**P=0.029**	P=0.270
Q_{CCA} (mL·min^{-1})	451±40	499±72*	424±65	538±78*	**P=0.003**	P=0.760	P=0.165

Abbreviations: End-tidal PCO_2, $P_{ET}CO_2$; end-tidal PO_2, $P_{ET}O_2$; ventilation, $\dot{V}_E$; tidal volume, V_T; respiratory rate, RR; mean arterial pressure, MAP; systolic blood pressure, SBP; diastolic blood pressure, DBP; cardiac output, CO; heart rate, HR; stroke volume, SV; Q_{CCA}, common carotid artery blood flow. *P<0.05 time effect; $^{+}$P<0.05 condition effect; $^{\#}$EX significantly different than HS; $^{\$}$PRE-EX significantly different than EX; $^{\%}$PRE-HS significantly different than HS. Data are mean ± SD for n=11. Data were compared with a linear mixed effects model including fixed factors of time (PRE vs. *during*) and condition (EX vs. HS) and random effects for subject ID.

Table 2. Absolute vascular parameters at rest (PRE) and during submaximal exercise (EX) and passive heat stress (HS)

	PRE-EX	EX	PRE-HS	HS	*P-Values*		
ICA					*Time*	*Condition*	*Time*Condition*
Diameter (cm)	0.49±0.04	0.51±0.05	0.49±0.03	0.50±0.03	P=0.140	P=0.776	P=0.909
Velocity ($cm \cdot s^{-1}$)	40.83±4.11	41.98±8.01	42.66±4.72	46.99±6.67	P=0.129	P=0.057	P=0.394
$\dot{Q}$ ($mL \cdot min^{-1}$)	237±48	256±79	246±41	278±60	P=0.104	P=0.329	P=0.665
Shear Rate (s^{-1})	332±42	335±67	347±40^{+}	378±51^{+}	P=0.234	**P=0.030**	P=0.342
SRAUC (a.u.)	19936±2531	20107±4004	20817±2392^{+}	22656±3077^{+}	P=0.223	**P=0.022**	P=0.336
CVC ($mL \cdot min^{-1} \cdot mmHg^{-1}$)	2.68±0.63	2.70±0.77	2.81±0.51	3.20±0.64	P=0.200	P=0.052	P=0.242
ECA							
Diameter (cm)	0.45±0.04	0.48±0.04*	0.45±0.05	0.47±0.05*	**P=0.004**	P=0.706	P=0.722
Velocity ($cm \cdot s^{-1}$)	27.13±7.02	31.93±10.87*	25.24±5.13	35.18±6.91*	**P<0.001**	P=0.675	P=0.169
$\dot{Q}$ ($mL \cdot min^{-1}$)	137±44	189±86*	137±61	198±67*	**P<0.001**	P=0.628	P=0.618
Shear Rate (s^{-1})	240±64	259±84*	220±41	290±56*	**P=0.018**	P=0.763	P=0.188
SRAUC (a.u.)	14392±3856	15550±5017*	13217±2480	17400±3365*	**P=0.018**	P=0.767	P=0.189
CVC ($mL \cdot min^{-1} \cdot mmHg^{-1}$)	1.53±0.46	2.04±0.94*	1.54±0.62	2.27±0.71*	**P<0.001**	P=0.222	P=0.268
VA							
Diameter (cm)	0.41±0.04	0.42±0.06	0.41±0.04	0.41±0.05	P=0.299	P=0.613	P=0.387
Velocity ($cm \cdot s^{-1}$)	25.27±3.82	27.70±5.71*	24.34±5.05	28.05±5.04*	**P=0.016**	P=0.793	P=0.569
$\dot{Q}$ ($mL \cdot min^{-1}$)	106±29	122±41*	101±27	120±35*	**P=0.006**	P=0.514	P=0.785
Shear Rate (s^{-1})	243±32	263±52*	235±52	268±45*	**P=0.027**	P=0.871	P=0.564
SRAUC (a.u.)	14572±1918	15798±3125*	14099±3131	16059±2699*	**P=0.027**	P=0.867	P=0.565
CVC ($mL \cdot min^{-1} \cdot mmHg^{-1}$)	1.18±0.29	1.27±0.40	1.14±0.28	1.40±0.40	**P=0.008**	P=0.466	P=0.168
MCAv ($cm \cdot s^{-1}$)	59.77±11.48$^{\$}$	69.05±11.25$^{\#\$}$	62.81±12.82	62.71±11.54$^{\#}$	**P=0.027**	P=0.274	**P=0.009**
MCA_{CVC} ($cm \cdot s^{-1} \cdot mmHg^{-1}$)	0.67±0.12	0.73±0.12	0.72±0.14	0.73±0.17	P=0.209	P=0.415	P=0.456
PCAv ($cm \cdot s^{-1}$)	42.30±8.30$^{\$}$	47.64±9.84$^{\#\$}$	43.06±9.32	42.09±9.53$^{\#}$	P=0.130	**P=0.007**	**P=0.024**
PCA_{CVC} ($cm \cdot s^{-1} \cdot mmHg^{-1}$)	0.47±0.08	0.51±0.10	0.49±0.09	0.50±0.15	P=0.262	P=0.554	P=0.556
gCBF ($mL \cdot min^{-1}$)	692±96	774±216*	689±88	791±132*	**P=0.029**	P=0.869	P=0.800
gCVC ($mL \cdot min^{-1} \cdot mmHg^{-1}$)	7.81±1.28	8.09±2.08*	7.83±0.99	9.25±1.15*	**P=0.027**	P=0.144	P=0.157

Abbreviations: Internal carotid artery, ICA; external carotid artery, ECA; vertebral artery, VA; middle cerebral artery mean velocity, MCA*v*; posterior cerebral artery mean velocity, PCA*v*; flow, *Q*; shear rate area under the curve, SRAUC; cerebrovascular conductance, CVC; global, *g*; cerebral blood flow, CBF. *P<0.05 time effect; $^{+}$P<0.05 condition effect; $^{\#}$EX significantly different than HS; $^{\$}$PRE-EX significantly different than EX. Data are mean ± SD for n=11. Data were compared with a linear mixed effects model including fixed factors of time (PRE vs. *during*) and condition (EX vs. HS) and random effects for subject ID.

Table 3. Neurovascular coupling (NVC) at rest (PRE) and during submaximal exercise (EX) and passive heat stress (HS)

		PRE-EX	EX	PRE-HS	HS	*P-Values*		
NVC Response						*Time*	*Condition*	*Time*Condition*
Peak absolute ($cm \cdot s^{-1}$)	PCA*v*	48.22±11.13	54.70±11.13	46.78±10.92^{+}	47.29±11.11^{+}	P=0.064	**P=0.024**	P=0.110
	PCA_{CVC}	0.54±0.14	0.63±0.14*	0.56±0.14	0.58±0.14*	**P=0.035**	P=0.471	P=0.180
Δ Peak absolute ($cm \cdot s^{-1}$)	PCA*v*	9.35±2.98	9.02±2.98	8.06±2.88^{+}	7.20±2.97^{+}	P=0.366	**P=0.025**	P=0.685
	PCA_{CVC}	0.11±0.03	0.12±0.03	0.10±0.03^{+}	0.10±0.03^{+}	P=0.372	**P=0.035**	P=0.418
Average absolute ($cm \cdot s^{-1}$)	PCA*v*	42.66±9.67	48.79±9.67*	41.61±9.49^{+}	42.39±9.65*$^{+}$	**P=0.031**	**P=0.023**	P=0.089
	PCA_{CVC}	0.48±0.12	0.55±0.12	0.49±0.12	0.51±0.12	P=0.055	P=0.543	P=0.228
Δ Average absolute ($cm \cdot s^{-1}$)	PCA*v*	3.80±1.49	3.13±1.49	2.88±1.44^{+}	2.31±1.49^{+}	P=0.087	**P=0.021**	P=0.893
	PCA_{CVC}	0.04±0.02	0.04±0.02	0.03±0.02^{+}	0.03±0.02^{+}	P=0.521	**P=0.018**	P=0.928
Peak relative (%)	PCA*v*	24.35±5.69	19.57±5.69*	20.89±5.45	17.98±5.68*	**P=0.014**	P=0.100	P=0.532
	PCA_{CVC}	24.99±5.05	23.35±5.05	21.70±4.86^{+}	20.54±5.05^{+}	P=0.265	**P=0.021**	P=0.849
Average relative (%)	PCA*v*	10.07±3.47	6.72±3.47*	7.57±3.32	5.76±3.47*	**P=0.009**	P=0.070	P=0.406
	PCA_{CVC}	9.85±3.21	7.70±3.21	7.10±3.07^{+}	6.13±3.21^{+}	P=0.078	**P=0.017**	P=0.488
Time to peak (s)	PCA*v*	11.85±5.95	13.97±5.95	13.42±5.68	13.35±5.95	P=0.578	P=0.794	P=0.554
	PCA_{CVC}	11.94±6.43	14.66±6.43	14.95±6.14	13.49±6.43	P=0.728	P=0.615	P=0.254

*P<0.05 time effect; $^{+}$P<0.05 condition effect. Data are mean ± SD for n=11. Data were compared with a linear mixed effects model including fixed factors of time (PRE vs. *during*) and condition (EX vs. HS) and random effects for subject ID.

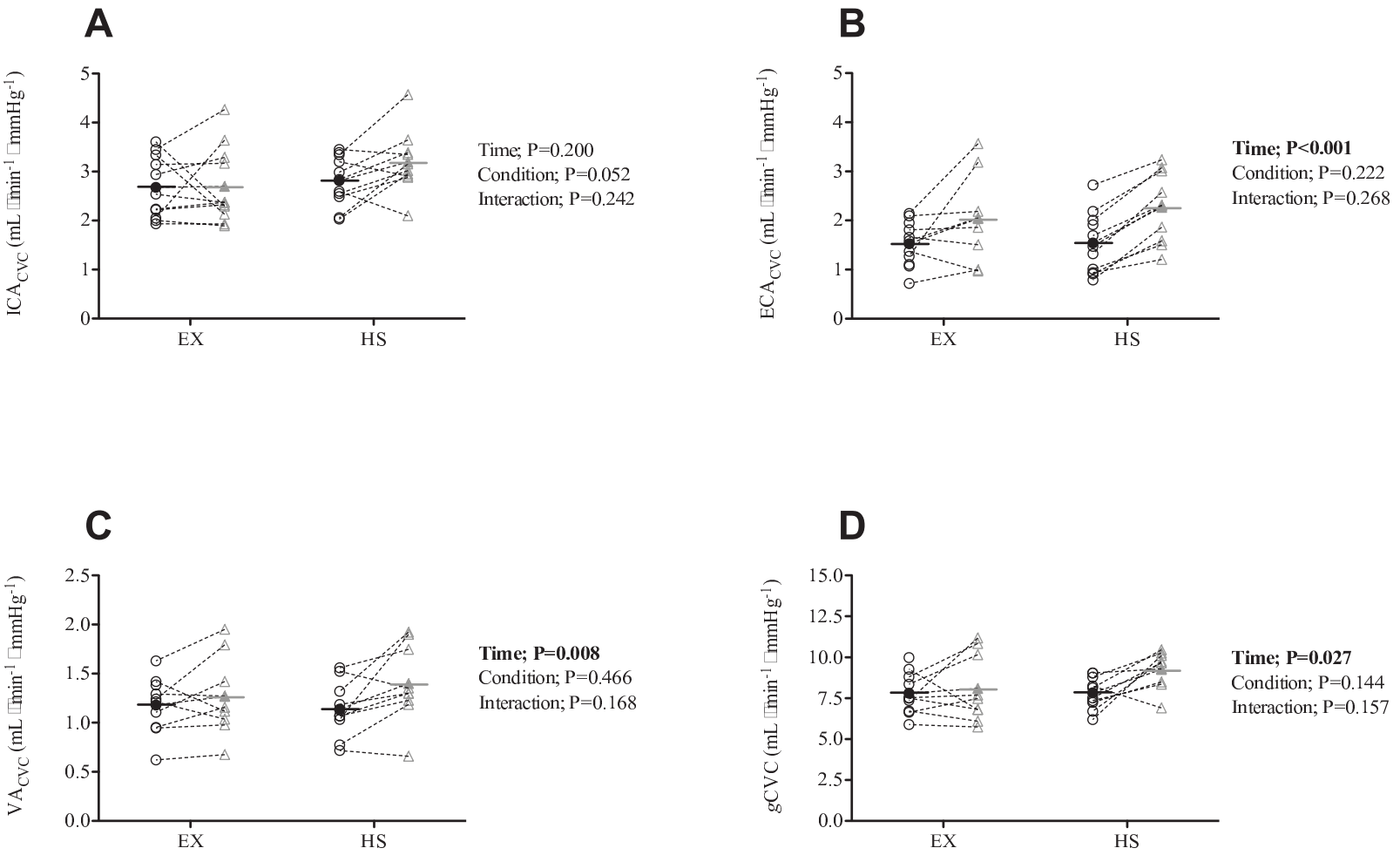

Figure 1. Cerebrovascular conductance (CVC) before (blue circles) and during (red triangles) submaximal exercise (EX) and temperature-matched passive heat stress (HS). A) Internal carotid artery (ICA); B) External carotid artery (ECA); C) Vertebral artery (VA); D) global (*g*; i.e., 2x ICA+VA). The ECA_{CVC}, VA_{CVC}, and *g*CVC were all increased to the same extent during EX and HS

conditions (time effect: all $P<0.05$). Data are individual values with group average for n=11. Data were compared with a linear mixed effects model including fixed factors of time (PRE vs. *during*) and condition (EX vs. HS) and random effects for subject ID.

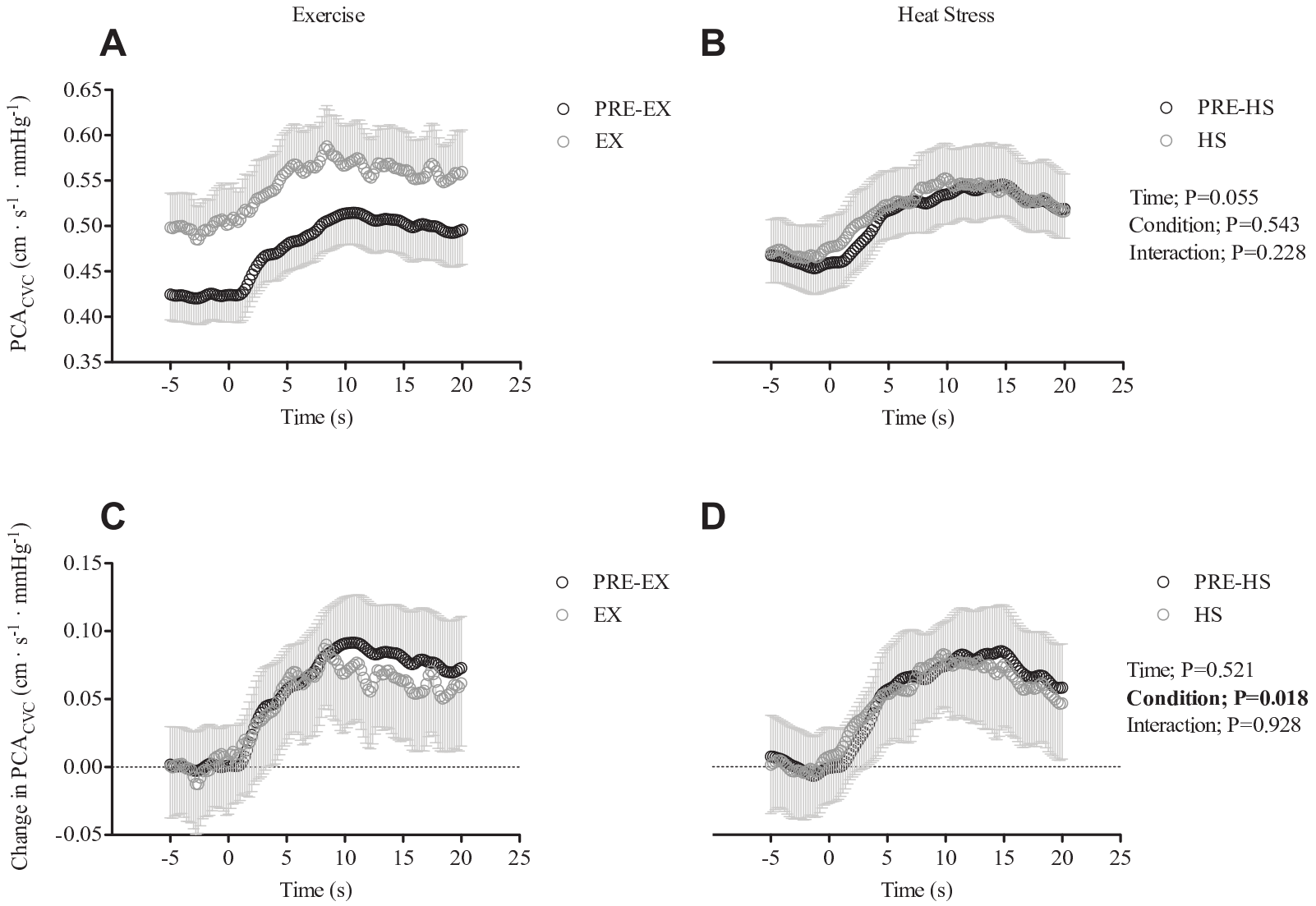

Figure 2. Absolute neurovascular coupling response of the posterior cerebral artery cerebrovascular conductance (PCA$_{CVC}$) before

(PRE) and during submaximal exercise (EX; A & C) and temperature-matched passive heat stress (HS; B & D). A & B) Average absolute change in PCA_{CVC}; C & D) Absolute change from BL in PCA_{CVC}. Absolute PCA_{CVC} was elevated during EX; therefore, the average absolute change in PCA_{CVC} was significantly higher with EX (A). When expressed as an absolute *change* score, this response was higher on average for the EX condition (C vs. D). Data are mean ± SEM for n=11. Data were compared with a linear mixed effects model including fixed factors of time (PRE vs. *during*) and condition (EX vs. HS) and random effects for subject ID.

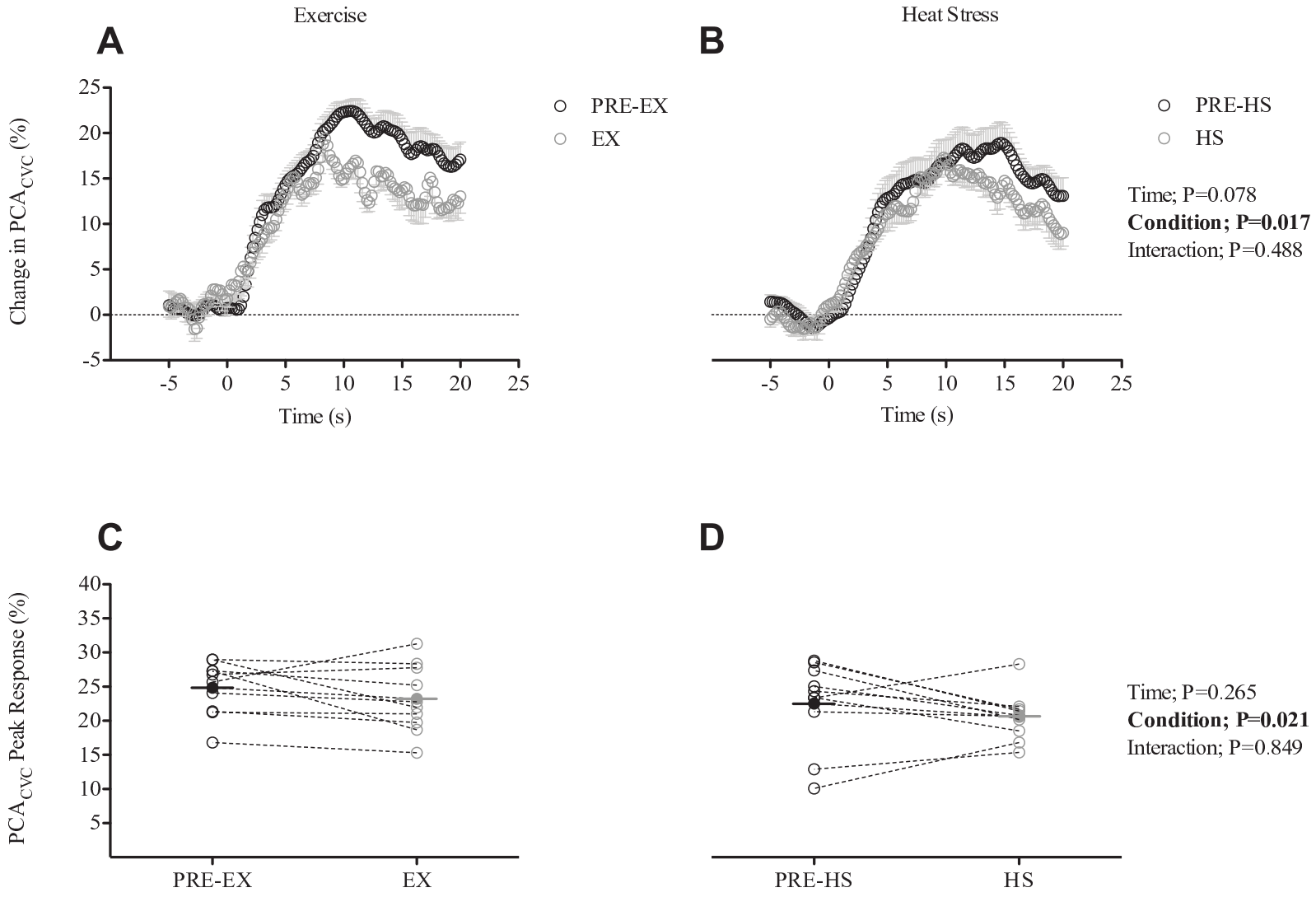

Figure 3. Neurovascular coupling response of the posterior cerebral artery cerebrovascular conductance (PCA_{CVC}) before (PRE) and

during submaximal exercise (EX; A & C) and temperature-matched passive heat stress (HS; B & D). A & B) Average relative change in PCA_{CVC}; C & D) Individual data with respective group average lines for relative peak response of PCA_{CVC}. As PCA_{CVC} was elevated at BL, the relative peak response was lower during EX; however, this condition was on average higher than the HS trial (A vs. B). Data are mean ± SEM for n=11. Data were compared with a linear mixed effects model including fixed factors of time (PRE vs. *during*) and condition (EX vs. HS) and random effects for subject ID.

A
ICA$_{CVC}$ (mL · min^{-1} · mmHg^{-1})
Time; P=0.200
Condition; P=0.052
Interaction; P=0.242
EX
HS
B
ECA$_{CVC}$ (mL · min^{-1} · mmHg^{-1})
Time; P<0.001
Condition; P=0.222
Interaction; P=0.268
EX
HS
C
VA$_{CVC}$ (mL · min^{-1} · mmHg^{-1})
Time; P=0.008
Condition; P=0.466
Interaction; P=0.168
EX
HS
D
gCVC (mL · min^{-1} · mmHg^{-1})
Time; P=0.027
Condition; P=0.144
Interaction; P=0.157
EX
HS

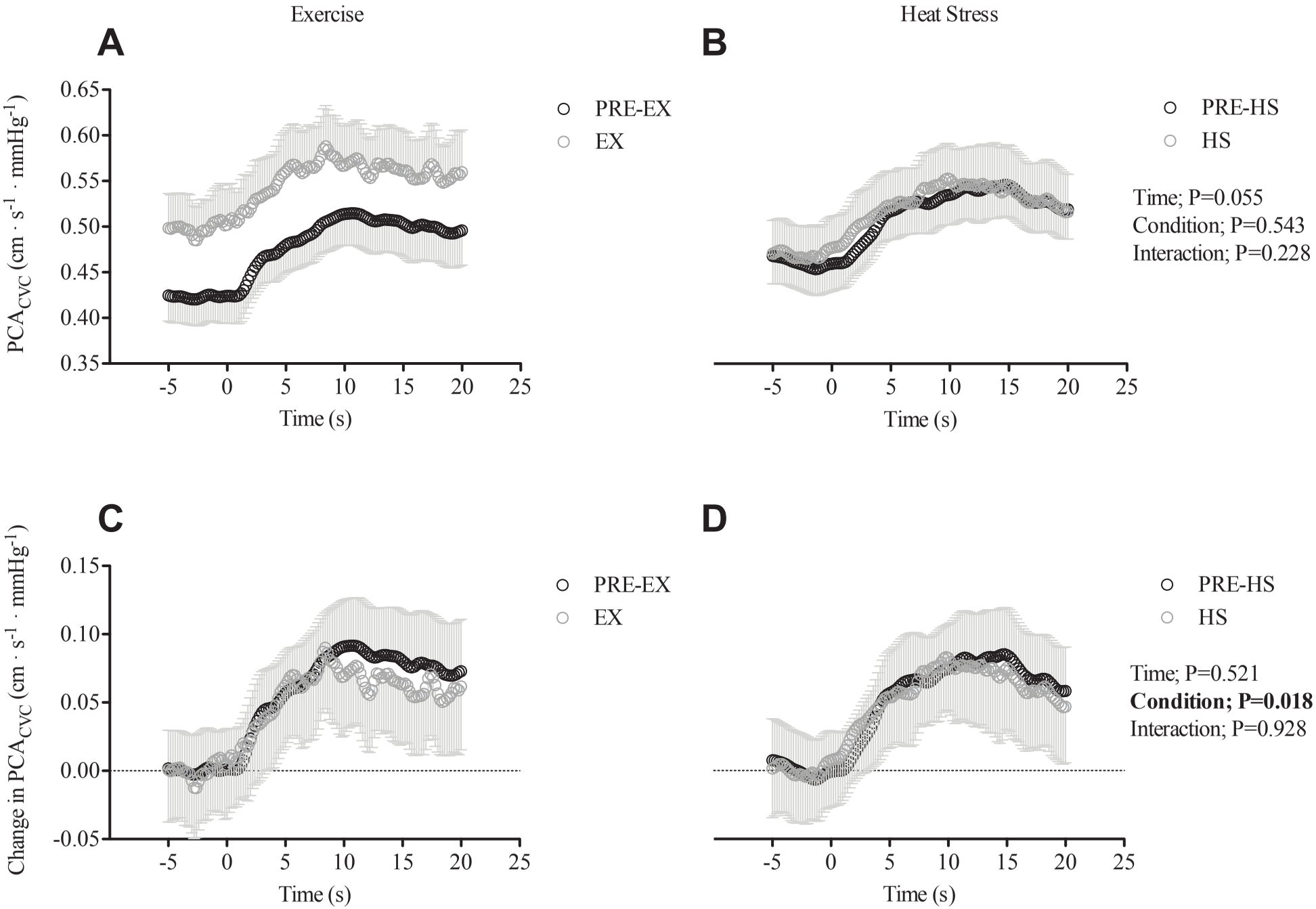
Exercise
Heat Stress
A
B
C
D
PCA$_{CVC}$ (cm · s^{-1} · mmHg^{-1})
Change in PCA$_{CVC}$ (cm · s^{-1} · mmHg^{-1})
0.65
0.60
0.55
0.50
0.45
0.40
0.35
0.15
0.10
0.05
0.00
-0.05
-5
0
5
10
15
20
25
Time (s)
PRE-EX
EX
PRE-HS
HS
Time; P=0.055
Condition; P=0.543
Interaction; P=0.228
Time; P=0.521
Condition; P=0.018
Interaction; P=0.928

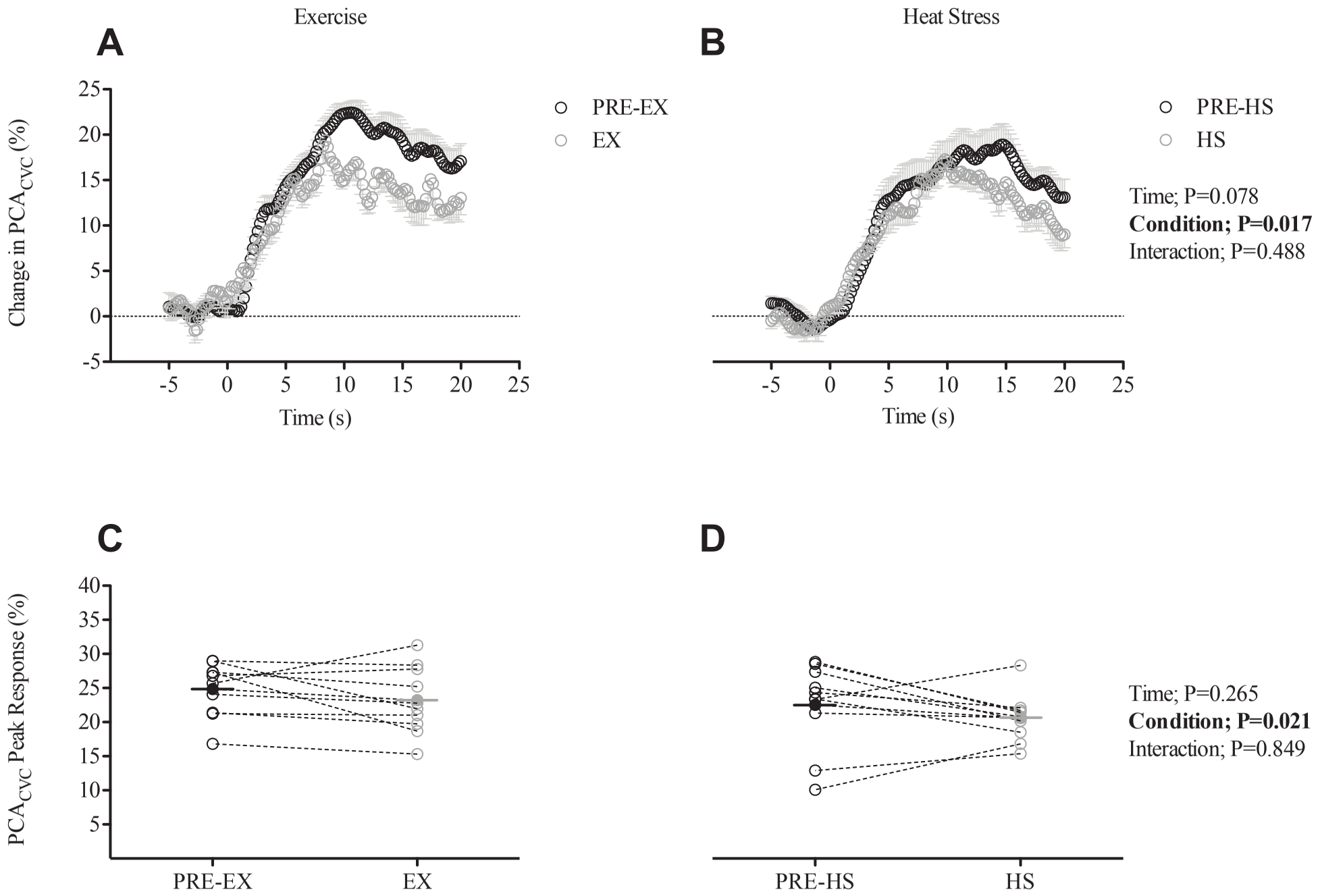
Exercise
A
Change in PCA$_{CVC}$ (%)
25
20
15
10
5
0
-5
-5
0
5
10
15
20
25
Time (s)
PRE-EX
EX
Heat Stress
B
PRE-HS
HS
Time; P=0.078
Condition; P=0.017
Interaction; P=0.488
C
PCA$_{CVC}$ Peak Response (%)
40
35
30
25
20
15
10
5
PRE-EX
EX
D
PRE-HS
HS
Time; P=0.265
Condition; P=0.021
Interaction; P=0.849